50th Lunar and Planetary Science Conference 2019 (LPI Contrib. No. 2132)

1981.pdf

SAPONITE DISSOLUTION EXPERIMENTS AND IMPLICATIONS FOR MARS. N. C. Luu[1], E. M. Hausrath[1], A. M. Sanchez[1], S. Gainey[2], E. Rampe[3], T. Peretyazhko[3], O. Tschauner[1], A. Lanzirotti[4], C. Adcock[1], and K. Leftwich[5], [1]Department of Geoscience, University of Nevada, Las Vegas, Las Vegas, NV, USA (luun1@unlv.nevada.edu), [2]College of Engineering, University of Nevada, Las Vegas, Las Vegas, NV, USA [3]NASA Johnson Space Center, Houston, TX, USA [4]Center for Advanced Radiation Sources, Univ. of Chicago, Chicago, IL, USA, [5]Proto, Taylor, MI, USA.

Introduction: Recent work suggests that the mineralogical sequence of the Murray formation at Gale crater may have resulted from diagenetic alteration after sedimentation [1], or deposition in a stratified lake with oxic surface and anoxic bottom waters [2]. Fe-containing clay minerals are common both at Gale crater, and throughout the Noachian-aged terrains on Mars. These clay minerals are primarily ferric (Fe^{3+}), and previous work suggests that these ferric clay minerals may result from alteration of ferrous (Fe^{2+}) smectites that were oxidized after deposition [3]. The detection of trioctahedral smectites at Gale crater by CheMin suggests Fe^{2+} smectite was also deposited during the early Hesperian [5].

However, due to their sensitivity to oxygen, Fe^{2+} smectites are difficult to analyze on Earth [3] and very few saponite dissolution rates exist in the literature [4]. To the best of our knowledge, no experiments have measured the dissolution rates of ferrous saponites under oxidizing and reducing conditions. In order to better understand the characteristics of water-rock interaction at Gale crater, particularly the oxidation state, we report our results to date on ongoing syntheses of ferrous and magnesian saponites and dissolution experiments of natural saponite [5] under ambient conditions. Future experiments will include the dissolution of synthetic ferric, ferrous, and magnesian saponites under oxidizing and anoxic conditions at a range of pH values.

Methods:

Synthesis of Fe-Mg saponites: Fe-Mg saponites are being synthesized under anoxic conditions in a PlasLabs glovebox filled with high-purity nitrogen following methods modified from [6]. Prior to use, all solutions are bubbled with high purity nitrogen. To ensure reducing conditions during synthesis, 4.2g of sodium dithionite is added to the solution mix prior to the addition of 19.8 mL of NaOH to cause precipitation of the saponite precursor. The final suspended mixture is cured for 24-hours in the glovebox. The solution and precipitate are rigorously hand-shaken before loading into Teflon-lined Parr vessels and sealed within the glovebox then transferred to an oven at 150 ºC and heated for 48-hours. Vessels are removed, cooled, and transferred into the glove box where the supernatant is decanted, and the pH of supernatant measured. Precipitated material is rinsed by placing the material in 50 ml centrifuge tubes sealed with O-rings to prevent oxidation. Centrifuge tubes are

then returned to the anoxic glovebox where the supernatant is decanted and rinsed with deoxygenated 18.2 MΩ deionized water. Rinsed samples are returned to the glove box, placed in an N_2-filled desiccator, sealed, removed from the glovebox, and placed under vacuum until dried. Final material is returned to the glovebox where it is ground to a powder and stored until use. Synthesis of the pure Mg-saponite end-member followed the same methods as described above, but all steps were performed under ambient lab conditions since Mg is not redox sensitive.

Preparation of natural saponite: For comparison, we are also using a terrestrial ferrosaponite from Griffith Park, CA [5]. This ferrosaponite shares similar characteristics to the smectites found at Yellowknife Bay at Gale crater and may have a similar depositional history to Martian smectites formed during the Noachian [7]. The saponite was collected from Griffith Park, California, and the pockets of saponite identified, and extracted using a dental pick. The saponite was powdered, sieved to retain the 150-45 µm size fraction, and used in dissolution experiments.

Batch dissolution experiments: Batch dissolution experiments were performed after [8]. In each case, 250 mL of solution was added to 0.5 g of mineral. Solutions contained 0.01 M NaCl to prevent large changes in activity of water as the mineral dissolves, and were acidified with OmniTrace nitric acid to the desired pH. All solutions were made using 18.2 MΩ deionized water, and the solution temperature was equilibrated to 25 °C before adding it to the mineral. Experiments were performed at 25 ± 0.1 ºC in a temperature-controlled shaking water bath. Each experimental condition was performed in duplicate with a blank. Experiments were sampled 2-3 times per day for one week, and then after approximately 1 month, a second set of samples was collected to assess steady state conditions.

Analyses of solid and solution samples: Silica concentrations were measured using an Atomic Absorption Spectrometer (Thermo Scientific iCE 3000 series). Solution concentrations were corrected for changes in batch volume due to sampling after [8].

Powder X-ray diffraction (XRD) patterns were collected for all synthetic and natural samples using a Proto AXRD Benchtop Powder X-ray Diffractometer with a Cu X-ray tube. Fe-containing synthetic samples were loaded onto the sample holder and secured with Kapton

tape in the N_2-filled glove box, transported to the X-ray diffractometer in an airtight N_2-filled pelican box, and then immediately analyzed under ambient conditions.

Unreacted and reacted minerals were also analyzed by synchrotron μXRD and Fe K-edge X-ray Absorption Near Edge Structure (XANES) spectroscopy at the Advanced Photon Source (APS) beamline 13-IDE. Samples were transported to the APS in an airtight N_2-filled pelican box and analyzed quickly after removal. Preliminary Fe K-edge centroid fits were normalized with the Lorentzian function using Larch [9].

Results and Discussion: Silica concentrations collected during the first week of sampling showed nonlinear behavior indicative of approach to steady state or equilibrium where a precipitation reaction is important (Figure 1). The apparent dissolution rate constant was therefore calculated after [10] and [8] using equation 2:

$$-m_{ss} \ln\left(1 - \frac{m}{m_{ss}}\right) = Ak_{diss}t + C \qquad (1)$$

where m is moles of silica released at each sampling point, m_{ss} is moles released at steady state (based on the average of the last two long term point(s)), A is the surface area, k_{diss} is the apparent dissolution rate constant in mol m^{-2} s^{-1}, t is time in seconds, and C is the constant of integration and allowed to be nonzero.

Results indicate that saponite dissolution rates are faster under more acidic conditions (Figure 1), and faster than similar layer silicates such as nontronite and montmorillonite under similar pH conditions [11].
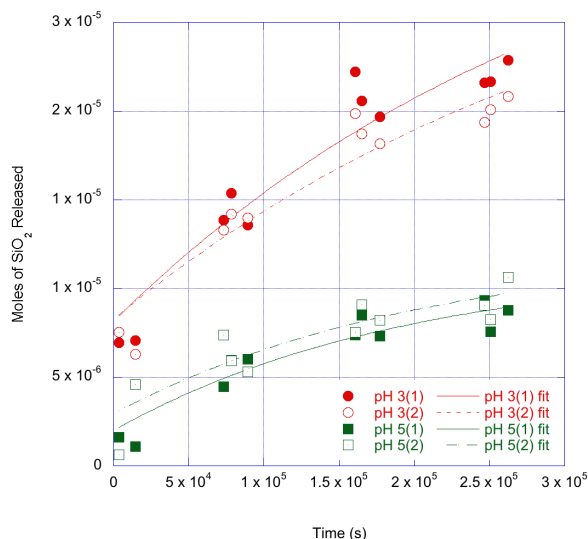

Figure 1. Silica release versus time for saponite dissolution fit with equation (1) as described in the text.

Preliminary centroid fits of Fe K-edge XANES suggest that the natural saponite contains both ferrous and ferric Fe, consistent with previous results [4], and the saponite reacted at pH 3 shows a shift to higher energy,

consistent with oxidation occurring under our dissolution experiments performed under ambient conditions or preferential dissolution of ferrous phases leaving ferric phases remaining in the reacted material (Figure 2). In comparison, our synthetic 100-Fe is the most reduced of the four samples.
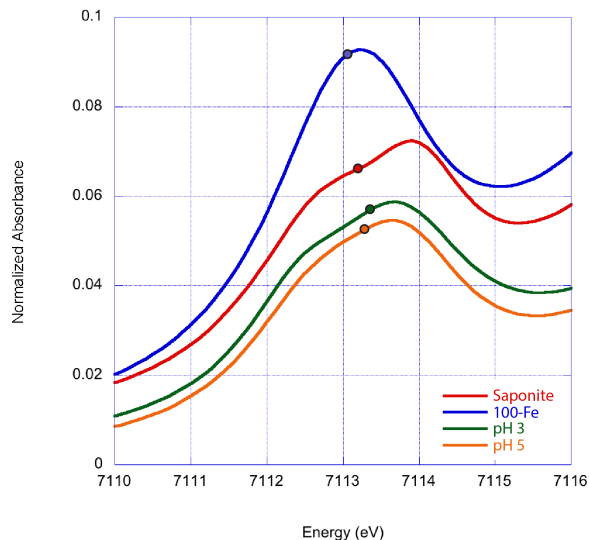

Figure 2. Fe K-edge XANES with centroid fits marked on each curve with a circle for unreacted natural saponite (7113.20 eV) (labeled saponite on graph), natural saponite reacted at pH = 3 (7113.35 eV) (labeled pH 3), natural saponite reacted at pH = 5 (7113.28 eV) (labeled pH 5), and the ferrous Fe syntheses (7113.06 eV) (labeled 100-Fe).

References: [1] Rampe, E. B. et al. (2017) *EPSL*, *471*, 172-185. [2] Hurowitz, J. A. et al. (2017) *Science*, *356*(6341), eaah6849. [3] Chemtob, S. M. et al. (2015) *JGR: Planets*, *120*(6), 1119-1140. [4] Brigatti, M. et al. (1999) *Clay Minerals*, *34*(637-645). [5] Treiman, A. H. et al. (2014) *American Mineralogist*, *99*(11-12), 2234-2250. [6] Gainey, S. R. et al. (2017) *Nature Communications*, *8*(1), 1230. [7] Chemtob, S. M. et al. (2017) *JGR: Planets*, *122*(12), 2469-2488. [8] Steiner, M. H. et al. (2016) *GCA*, *195*, 259-276. [9] Newville, M. (2013) *Journal of Physics: Conference Series, 430.* [10] Hausrath, E. M. and Brantley, S. L. (2010) *JGR: Planets, 115*(E12). [11] Gainey, S. R. et al. (2014) *GCA, 126*(192-211).